Rectified motion in an asymmetrically structured channel due to induced-charge electrokinetic and thermo-kinetic phenomena

Cite as: Phys. Fluids **28**, 022004 (2016); https://doi.org/10.1063/1.4941300
Submitted: 05 August 2015 . Accepted: 19 January 2016 . Published Online: 08 February 2016

Hideyuki Sugioka

PHYSICS OF FLUIDS **28**, 022004 (2016)

Rectified motion in an asymmetrically structured channel due to induced-charge electrokinetic and thermo-kinetic phenomena

Hideyuki Sugioka[a)]
Frontier Research Center, Canon Inc. 30-2, Shimomaruko 3-chome, Ohta-ku, Tokyo 146-8501, Japan and Department of Mechanical Systems Engineering, Shinshu University 4-17-1 Wakasato, Nagano 380-8553, Japan

(Received 5 August 2015; accepted 19 January 2016; published online 8 February 2016)

It would be advantageous to move fluid by the gradient of random thermal noises that are omnipresent in the natural world. To achieve this motion, we propose a rectifier that uses a thermal noise along with induced-charge electroosmosis and electrophoresis (ICEO and ICEP) around a metal post cylinder in an asymmetrically structured channel and numerically examine its rectification performance. By the boundary element method combined with the thin double layer approximation, we find that rectified motion occurs in the asymmetrically structured channel due to ICEO and ICEP. Further, by thermodynamical and equivalent circuit methods, we discuss a thermal voltage that drives a rectifier consisting of a fluidic channel of an electrolyte and an impedance as a noise source. Our calculations show that fluid can be moved in the asymmetrically structured channel by the fluctuation of electric fields due to a thermal noise only when there is a temperature difference. In addition, our simple noise argument provides a different perspective for the thermo-kinetic phenomena (around a metal post) which was predicted based on the electrolyte Seebeck effect in our previous paper [H. Sugioka, "Nonlinear thermokinetic phenomena due to the Seebeck effect," Langmuir **30**, 8621 (2014)]. © *2016 AIP Publishing LLC.* [http://dx.doi.org/10.1063/1.4941300]

I. INTRODUCTION

Random noises are omnipresent in the world. Thus, it would be advantageous to move something by using these noises. Although there is no ambiguity for macroscopic signals as the waves of the sea can generate a net electric power, care is needed in applying the concept of rectification to signals of the order of magnitude of thermal noise. On one hand, as for an electric diode, many researchers have already explored this problem. Theoretically, Brillouin[1] has shown that, to satisfy the second law of thermodynamics, a diode at finite temperature must generate a dc signal which compensates the current resulting from the rectification of thermal noise. Experimentally, Gunn and Staples[2] have shown that this signal should actually be observable as a spontaneous reverse current when the diode is connected to resistor at a lower temperature itself. Further, Callegaro and Pisani[3] have shown that a realization of Nyquist's gedanken experiment[4] is feasible and that direct measurement of noise power flowing in the line that connects two resistors is possible. On the other hand, as for a fluidic diode, many researchers also have studied the concept of "force-free" motion under the names "rectification," "Brownian motor," and "Feynman ratchet."[5–10] In this context, Silberzan *et al.*[9] have observed the rectified motion ($\sim\mu$m/s with $\sim 10^4$ V/m) of colloidal beads in an asymmetrically structured channel (so-called ratchet-shaped channel) whose lateral dimension exhibits a modulation in width whose shape is periodic and polar along its axis under the fluctuation due to dielectrophoresis (DEP) by applying ac electric fields. Further, Groisman and Quake[11] have

a)Electronic mail: hsugioka@shinshu-u.ac.jp

shown that a 0.01% aqueous solution of a high molecular weight polymer also exhibits a rectified motion in such a ratchet-shaped channel. Of course, more generally, the movement of colloidal particle under the temperature gradient is well known in terms of thermo-phoresis or thermo-kinetic phenomena;[12] however, above mentioned studies provide a different viewpoint.

Recently, it has been recognized that conductors in an ionic solution with a broken symmetry generate a large net flow velocity (~mm/s in an electric field of approximately 10^4 V/m) due to induced-charge electrokinetic phenomena, which include induced-charge electroosmosis or electrophoresis (ICEO/ICEP).[13–21] ICEO/ICEP is different from the classical electroosmosis and electrophoresis because it results from the interaction between an electric field and ions in an electric double layer formed by the polarizing effect of the electric field itself. It should be noted that it can be expected to avoid the electro-chemical problems associated with dc electric fields and to achieve the high slip velocity due to the nonlinear relation ($U_0 \propto E_0^2$). In addition, in our previous paper, we predicted quadrupolar thermo-kinetic flows around a metal cylinder under the existence of the temperature gradient.[22] However, thus far, it has not been clarified how much flow an ICEP or ICEO pump exhibits by the signals of the order of magnitude of thermal noise. In this study, to answer the question that what is happening in an asymmetrically structured channel, we focus on the rectified motion in the ratchet shaped channel due to ICEO/ICEP and elucidate the possibility of achieving the motion by the thermal noise. Interestingly, we find that within the framework of the boundary element method combined with the thin double layer approximation, fluid can be moved in the asymmetrically structured channel by the fluctuation of electric fields due to thermal noise if there is a temperature difference between a fluid cell and a connected resistor.

II. THEORY

A. Geometry model

Figure 1 shows the schematic view of the basic component of the ICEO and ICEP rectifiers considered in this study. As shown in Fig. 1(a), we place a circular metal cylinder of radius c at the center of a funnel channel of length $L = 2.25w$, inlet width w ($=w_1 = 0.1$ μm), and outlet width w_2. Here, a metal cylinder in an ICEO rectifier is anchored to the substrate, whereas a metal cylinder in an ICEP rectifier can move in the channel. To consider the possibility of a fluidic rectification due to a thermal noise, we connect a large impedance $Z_1 = R_1 + jX_1$ at a high temperature T_1 to the electrodes of the ratchet channel, whose impedance is $Z_2 = R_2 + jX_2$ at a low temperature T_2 ($<T_1$), as shown in Fig. 1(a). Please note that $v_a(t)$ is an effective applied random noise voltage between the parallel electrodes of the fluidic channel in the time domain and $V_a(\omega)$ is a corresponding effective applied voltage in the frequency domain. Figure 1(b) shows an equivalent electrical circuit of the spontaneous rectifier. As shown in Fig. 1(b), we consider that the noise source element of Z_1 consists of a resistor of R_{10} and a parallelly connected capacitor of C_{10}. Further, as for the impedance of the fluidic rectifier of an electrolyte,[23] we consider a circuit consisting of a dc bulk resistance $R_{20} = w/\sigma_2 A$, a dc bulk capacitance $C_{20} = \epsilon A/w$, and a capacitance of a surface diffuse layer $C_s = \epsilon A/\lambda_D$, where λ_D ($\approx$1 nm) is the Debye screening length, $\sigma_2 = \epsilon D/\lambda_D^2$ is a bulk conductivity, D ($\approx 10^3$ μm^3/s) is the ionic diffusivity, A ($\approx w^2$) is an area of an electrode, ϵ ($\sim 80\epsilon_0$) is the dielectric permittivity of the solvent (typically water), and ϵ_0 is the vacuum permittivity. Here, although C_s may affect the cutoff frequency, we neglect it for simplicity, as a first attempt, since the important issue is just the mean square value of $v(t)$ which is approximately proportional to the bandwidth of the concerning electric circuit, as will be explain later; in this case, $Re\{Z_i\} = R_i(\omega) = R_{i0}/[1 + (\omega/\omega_{ci})^2]$ and $\mathrm{Im}\{Z_i\} = X_i(\omega) = -R_{i0}(\omega/\omega_{ci})/[1 + (\omega/\omega_{ci})^2]$, where ω_{ci} ($=1/R_{i0}C_{i0}$) is a cutoff frequency. Further, it is well known that the surface of a conductor has an equipotential; and Z_1 and Z_2 are connected by the ideal conductor of zero resistance; thus, there is no potential difference between Z_1 and Z_2.

B. Noise model for a single resistor

Figure 1(c) shows a noise model for a single resistor. As shown in Fig. 1(c), a thermal noise is not often shown explicitly, although we marked the resistor with a broken circle to differentiate

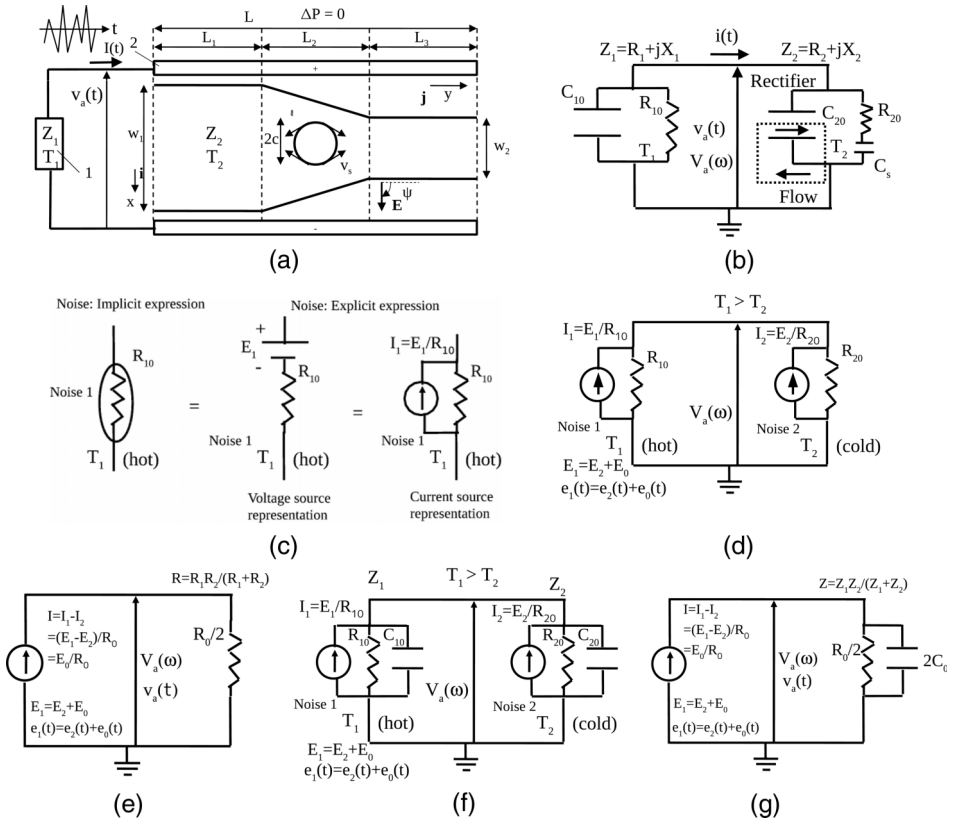

FIG. 1. Schematic view of ICEO and ICEP rectifiers. 1: random voltage source. 2: pair of electrodes. Here, length $L = 2.25w$, $L_1 = L_2 = L_3 = 0.75w$, and width $w = w_1 = 0.1$ μm. (a) Spontaneous rectifier. (b) Equivalent electrical circuit. (c) Noise model for a single resistor. (d) Two resistance noise model. (e) Equivalent electrical circuit for the resistance noise model. (f) Two impedance noise model. (g) Equivalent electrical circuit for the impedance noise model.

it from the simple resistor without a thermal noise. However, to describe the noise theory mathematically, we here use an explicit expression for a thermal noise, i.e., we consider a voltage source representation that consists of an internal resistance R_{10} and a voltage source E_1 in a serial manner or a current source representation that consists of an internal resistance R_{10} and a current source $I_1 = E_1/R_{10}$ in a parallel manner. Of course, it is well known that the voltage and current source representations can be replaced equivalently any time. Please note that only when there is no external circuit the potential difference between the both ends of the resistor is equivalent to E_1.

C. Noise model of two resistances for an effective mean square noise voltage

As the first step, as shown in Fig. 1(d), we consider the system that consists of two resistors (R_1 and R_2), which was considered in Refs. 3, 4, and 24, i.e., we neglect C_{10}, C_{20}, and C_s in Fig. 1(b); and in this case, $Z_1 = R_{10} = R_1$ and $Z_2 = R_{20} = R_2$. Although historically an electromotive force due to a thermal noise is not often drawn in the electric circuit model,[3,4,24] to clarify the problem, we consider an explicit current source $I_1 = E_1/R_{10}$ due to a thermal noise of R_{10} (=R_1) at a hot temperature T_1 in Fig. 1(d), while we consider an explicit current source $I_2 = E_2/R_{20}$ due to a thermal noise of R_{20} (=R_2) at a cold temperature T_2. Here, $E_i(\omega)$ ($e_i(t)$) is an electromotive force due to a thermal noise of R_{i0} in the frequency (time) domain. Namely, if the square of the noise voltage of R_i within the frequency interval $d\nu$ be denoted by $E_i^2 d\nu$, power that is transferred from R_i to R_j is represented by Nyquist's thermodynamical analysis[4] as

$$P_{i\to j} = \frac{E_i^2}{(R_i + R_j)^2} R_j d\nu = \frac{4kT_i R_i}{(R_i + R_j)^2} R_j, \tag{1}$$

where T_i is an absolute temperature of R_i and k is Boltzmann's constant. Thus, as described in Ref. 3 with an experimental fact, the net power that flows from the hot region (R_1) to the cold region (R_2) is

$$\bar{P} \equiv P_{1\to 2} - P_{2\to 1} = 4k\Delta T \frac{R_1 R_2}{(R_1 + R_2)^2}, \tag{2}$$

where ΔT ($\equiv T_1 - T_2$) is a temperature difference. Here, a net thermal and electric energy flows in the y direction for $\bar{P} > 0$ and $\Delta T > 0$, whereas a net thermal and electric energy flows in the $-y$ direction for $\bar{P} < 0$ and $\Delta T > 0$, in Fig. 1(c). Further, the maximum net power flow occurs at $R_1 = R_2 = R_0$. In this case, Eq. (2) gives

$$\bar{P}_{\max} = 4k\Delta T \frac{R_0 R_0}{(R_0 + R_0)^2} = k\Delta T. \tag{3}$$

Please note that Eq. (3) was experimentally examined by Callegaro and Pisani[3] and $\bar{P} = \bar{V}_a \bar{I}_{R_2} = \bar{V}_a \bar{V}_a / R_0$ (W/Hz) is the consumption power (W) per a unit frequency (Hz) at $R_{20} = R_0$, where $\bar{I}_{R_2} = \bar{V}_a / R_0$ is the current that flows in $R_2 = R_0$. Thus, for the two resistance noise model, it is obvious that

$$\bar{V}_a^2(\omega) = k\Delta T R_0, \tag{4}$$

$$\bar{v}_a^2(t) = k\Delta T R_0 W_{band}, \tag{5}$$

where W_{band} is a bandwidth of the concerning electric circuit, e.g., $W_{band} = \omega_c / 2\pi = 1/C_0 R_0$ for a parallel CR circuit in Fig. 1(e). Please note that Fig. 1(e) is an equivalent electrical circuit for the two resistance model at $R_1 = R_2 = R_0$. Here, we convert the electro-circuit in Fig. 1(d) to the electro-circuit in Fig. 1(d), by using the principle of superposition for an electrical circuit; and we believe that Fig. 1(e) helps the reader's understanding.

Of course, E_1 and E_2 are not equivalent to V_a even at $T_1 = T_2$. As is known well, to obtain the value of V_a, we need to consider the whole electro-circuit equation by considering the internal resistors R_1 and R_2 with the correct directions; and the fundamental equations of a thermal noise [i.e., Eqs. (1)–(3)] are derived in a similar manner. For example, when we consider $P_{1\to 2}$, we remove I_2 from Fig. 1(d) by using the principle of superposition for an electrical circuit; thus, we easily obtain the current that flows in R_2 as $I^{R_2} = \frac{R_1}{R_1+R_2}\frac{E_1}{R_1}$; further, the potential drop between the both ends of R_2 is calculated as $V^{R_2} = \frac{R_1 R_2}{R_1+R2}\frac{E_1}{R_1}$ since the combined resistance of R_1 and R_2 is $\frac{R_1 R_2}{R_1+R2}$ in Fig. 1(d); therefore, $P_{1\to 2} = E'\{V^{R_2} I^{R_2}\} = E'\{\frac{E_1^2 R_2}{(R_1+R2)^2}\} = \frac{4kTR_1R_2}{(R_1+R2)^2}$, where $E'\{x\}$ denotes the expectation value of x and we use $\bar{E}_1^2 = 4kTR_1$ [in Eq. (10)].

D. Noise model of two impedances for an effective mean square noise voltage

As the second step, we consider a two impedance noise system, which might be related to the thermo-kinetic phenomena, as shown in Fig. 1(f). Namely, as shown in Fig. 1(f), we consider an explicit current source I_1 ($=E_1/R_{10} = E_1/R_0$) due to a thermal noise of R_{10} ($=R_0$) at a hot temperature T_1 with a parallelly connected conductance of C_{10} ($=C_0$), while we consider an explicit current source $I_2 = E_2/R_{20} = E_2/R_0$ due to a thermal noise of R_{20} ($=R_0$) at a cold temperature T_2 with a parallelly connected conductance of C_{20} ($=C_0$). Here, as explained before, for $T_1 > T_2$, we can assume that

$$E_1(\omega) = E_2(\omega) + E_0(\omega), \tag{6}$$

$$e_1(t) = e_2(t) + e_0(t), \tag{7}$$

where $e_0(t)$ [E_0] is an excess noise voltage in the time (frequency) domain. Further, since $e_0(t)$ and $e_2(t)$ [$E_0(\omega)$ and $E_2(\omega)$] are the partial noises of $e_1(t)$ [$E_1(\omega)$], they are independent of each other and the average values should be zero, i.e., $\bar{e}_0 = \bar{e}_2 = 0$ and $\bar{E}_0 = \bar{E}_2 = 0$. Therefore, from Eqs. (6) and (7), for $T_1 > T_2$, we obtain that

$$\bar{E}_1^2 = E'\{(E_0 + E_2)^2\} = \bar{E}_2^2 + \bar{E}_0^2 + 2\bar{E}_1\bar{E}_2 = \bar{E}_2^2 + \bar{E}_0^2, \tag{8}$$

$$e_1^2 = e_2^2 + e_0^2. \tag{9}$$

Here, we use the ergodicity of the thermal noise. Further, since Eqs. (8) and (9) show the law of the conservation of energy, Eqs. (6) and (7) are justified physically. In addition, historically, Johnson[24] and Nyquist[4] clarified that

$$\bar{E}_1^2(\omega) = 4kT_1R_1, \tag{10}$$

$$\bar{E}_2^2(\omega) = 4kT_2R_2. \tag{11}$$

Thus, from Eqs. (8), (10), and (11), under the conditions that $T_1 > T_2$ and $R_1 = R_2 = R_0$, we obtain that

$$\bar{E}_0^2 = \bar{E}_1^2 - \bar{E}_2^2 = 4k(T_1 - T_2)R_0 = 4k\Delta TR_0. \tag{12}$$

Furthermore, since the electric circuit in Fig. 1(f) is converted to the electric circuit in Fig. 1(g) by using the principle of superposition, under the conditions that $R_{10} = R_{20} = R_0$ and $C_{10} = C_{20} = C_0$, the total current I and the total impedance Z are described by

$$I = I_1 - I_2 = \frac{E_1}{R_0} - \frac{E_2}{R_0} = (E_1 - E_2)/R_0 = E_0/R_0, \tag{13}$$

$$Z = \frac{Z_1Z_2}{Z_1 + Z_2} = \frac{1}{\frac{2}{R_0} + j\omega 2C_0} = \frac{R_0}{2}\frac{\mathrm{e}^{j\theta}}{\sqrt{1 + (\omega/\omega_c)^2}}. \tag{14}$$

Thus, we easily obtain that

$$V_a(\omega) = I(\omega)Z(\omega) = \frac{E_0}{R_0}\frac{R_0}{2}\frac{\mathrm{e}^{j\theta}}{\sqrt{1 + (\omega/\omega_c)^2}} = \frac{E_0(\omega)}{2}\frac{\mathrm{e}^{j\theta}}{\sqrt{1 + (\omega/\omega_c)^2}}. \tag{15}$$

Therefore,

$$V_a^2(\omega) = \frac{E_0^2(\omega)}{4}\frac{1}{1 + (\omega/\omega_c)^2}, \tag{16}$$

and the expectation value of $V_a^2(\omega)$ is described by

$$\bar{V}_a^2(\omega) = \frac{\bar{E}_0^2(\omega)}{4}\frac{1}{1 + (\omega/\omega_c)^2}. \tag{17}$$

Thus, by substituting Eq. (12) into Eq. (17), we obtain that

$$\bar{V}_a^2(\omega) = k\Delta TR_0\frac{1}{1 + (\omega/\omega_c)^2}. \tag{18}$$

Here, please note that, in detail, $\bar{v}_a^2(t)$ is defined as

$$\bar{v}_a^2(t) \equiv \lim_{T\to\infty}\frac{1}{T}\int_{-T/2}^{+T/2} v_a^2(t)dt = \int_{-\infty}^{+\infty}\lim_{T\to\infty}\frac{|V_T(\omega)|}{T}\frac{d\omega}{2\pi} = \int_0^{+\infty}\bar{V}_a^2(\omega)\frac{d\omega}{2\pi}, \tag{19}$$

where $\lim_{T\to\infty}\frac{|V_T(\omega)|}{T}$ is a power spectral density function and $\bar{V}_a$ is a effective mean square value of the applied voltage between electrodes; and in Eq. (19), we use the Parseval's theorem. Thus, by integrating the above equation over the frequency, we obtain $\bar{v}_a^2(t)$, i.e.,

$$\bar{v}_a^2(t) = k\Delta TR_0\int_{\omega=0}^{\omega=\infty}\frac{1}{1 + (\omega/\omega_c)^2}\frac{d\omega}{2\pi} = k\Delta TR_0\frac{\omega_c\pi}{2}\frac{1}{2\pi} = k\Delta TR_0\frac{1}{4R_0C_0} = \frac{k\Delta T}{4C_0}, \tag{20}$$

where $\omega_c = 1/R_0C_0$ is a cutoff frequency under the conditions that $R_{10} = R_{20} = R_0$ and $C_{10} = C_{20} = C_0$; and we use that

$$\int_{\omega=0}^{\omega=\infty}\frac{1}{1 + (\omega/\omega_c)^2}d\omega = \omega_c\int_{x=0}^{x=\infty}\frac{1}{1 + x^2}dx = \omega_c[\tan^{-1}x]_{x=0}^{x=\infty} = \omega_c\frac{\pi}{2} = \frac{\pi}{2R_0C_0}. \tag{21}$$

Interestingly, since $\omega_c = 1/R_0C_0$, a mean square voltage $\bar{v}_a^2(t)$ is not related to R_0 ($=R_{10} = R_{20}$) but to C_0 ($=C_{10} = C_{20}$), i.e., large fluctuations of thermal voltages will occur without a large resistance

R_0. Instead of that, the capacitance value of C_0 is required to be small to obtain the large bandwidth W_{band} for the concerning electric circuit. Further, please note that the sign of $\bar{v}_a^2$ in Eq. (21) shows the flowing direction of the power and energy, i.e., the net positive power flows from the T_1 region to the T_2 region when $\bar{v}_a^2 > 0$ and $T_1 > T_2$, whereas the net positive power flows from the T_2 region to the T_1 region when $\bar{v}_a^2 < 0$ and $T_1 < T_2$. However, when we consider the simple variance of the applied voltage due to the thermal noise, the negative sign of $\bar{v}_a^2$ is not appropriate; thus, we need to re-define the simple mean square value of the applied voltage due to the thermal noise as

$$\bar{v}_{a,rms}^2 \equiv |\bar{v}_a^2| = \frac{k|\Delta T|}{4C_0}, \tag{22}$$

and the simple root mean square value is defined as

$$\bar{v}_{a,rms} \equiv \sqrt{|\bar{v}_a^2|} = \sqrt{\frac{k\Delta T}{4C_0}}. \tag{23}$$

Obviously, $\bar{v}_{a,rms}^2$ and $\bar{v}_{a,rms}$ are irrelevant to the sign of ΔT.

Surprisingly, concerning Eq. (22), some researchers may insist that "$\sqrt{\bar{e}_1^2}$ and $\sqrt{\bar{e}_2^2}$ are equivalent to $\bar{v}_a$ at $T_1 = T_2$ and thus $\bar{v}_a^2$ should be proportional to T_1 (not ΔT)"; however, this argument is a typical mistake by the researcher who does not know the concept of the internal resistance. Please check that the argument cannot work at $T_1 \neq T_2$ without violating the assumption that Z_1 and Z_2 are connected by the ideal conductor and it never derives the established equations in the field of a thermal noise [e.g., Eqs. (1), (10), and (11)]. Further, ΔT in Eq. (22) is due to the second law of thermodynamics. In other word, historically, Nyquist[4] clarified the characteristics of the thermal noise [e.g., $E_i = 4kT_iR_i$ in Eqs. (10) and (11)] based on the second law of thermodynamics. Thus, Eq. (22) is justified from the viewpoint of the second law of thermodynamics.

E. Expected ICEO flow velocity due to the thermal noise

According to Bazant and Squires,[13] the representative velocity of the ICEO flow around a metal cylinder of a radius c is described as

$$U_0 = \frac{\epsilon c E_a^2}{\mu}, \tag{24}$$

and we expect that an average flow velocity U_p at the inlet of an ICEO pump is proportional to U_0, where E_a is an applied electric field and μ (~1 mPa s) is the viscosity. Thus, from Eqs. (22) and (24), we obtain the expected ICEO flow velocity due to the thermal noise as

$$\bar{U}_0 = \frac{\epsilon c \bar{E}_{a,rms}^2}{\mu} = \frac{\epsilon c}{\mu w^2}\bar{v}_{a,rms}^2 = \frac{\epsilon c}{\mu w^2}\frac{k|\Delta T|}{4C_0}, \tag{25}$$

where $\bar{E}_{a,rms} = \bar{v}_{a,rms}/w$ is a mean square value of an expected electric field due to the thermal noise. It should be noted that different from the nonlinear thermokinetic phenomena,[22] the average flow velocity due to the thermal noise is proportional to $|\Delta T|$. For example, by setting $C_0 = \epsilon A/w$, $w = 0.1$ μm, $A = w^2$, $\epsilon = 80\epsilon_0$, $\Delta T = 116.2$, and $c = 0.2w$, we obtain $\bar{v}_{a,rms} = 2.38$ mV and $\bar{U}_0 = 8$ μm/s.

F. Flow model

We consider a 2D quasi-static Stokes flow without Brownian movement, i.e., we consider the limit in which the Reynolds number Re tends to zero and the Peclet number is infinite. We assume the posts of the circular cylinder to be polarizable in an electrolytic solution under a dc or ac electric field. The motion of the surrounding fluid must satisfy Stokes equations modified by the inclusion of electrical stress. However, by using matched asymptotic expansion,[25] we can reduce them to the classical Stokes equations as follows:

$$\mu\nabla^2\boldsymbol{v} - \nabla p = 0, \qquad \nabla\cdot\boldsymbol{v} = 0, \tag{26}$$

$$\text{on } S_{\mathrm{p}}^{+}: \quad \boldsymbol{v} = \boldsymbol{U} + \boldsymbol{\Omega}\times\boldsymbol{x} + \boldsymbol{v}_{\mathrm{s}}, \tag{27}$$

$$\boldsymbol{v}_{\mathrm{s}} = 2U_0 \sin 2(\psi+\varphi)\boldsymbol{t}, \tag{28}$$

$$\int_{S_{\mathrm{p}}^{+}} \boldsymbol{f}\,\mathrm{d}l + \boldsymbol{F}_t^{\mathrm{ext}} = 0, \qquad \int_{S_{\mathrm{p}}^{+}} \boldsymbol{x}\times\boldsymbol{f}\,\mathrm{d}l + \boldsymbol{T}_t^{\mathrm{ext}} = 0, \tag{29}$$

where S_{p}^{+} denotes the surface defined as the outer edge of the double layer, $\boldsymbol{U}$ is the translational velocity, $\boldsymbol{\Omega}$ is the rotational angular velocity, $\boldsymbol{f}$ is the traction vector, and $\boldsymbol{F}_t^{\mathrm{ext}}$ and $\boldsymbol{T}_t^{\mathrm{ext}}$ are the total external force and torque, respectively, on the elliptical metal cylinder. Further, $\boldsymbol{x}$ $(= -c\sin\varphi\,\boldsymbol{i} + c\cos\varphi\,\boldsymbol{j})$ is the surface position of metals parameterized by φ, $\boldsymbol{t}$ $(=-\cos\varphi\,\boldsymbol{i} - \sin\varphi\,\boldsymbol{j})$ is the tangential unit vector of the position, electric field $\boldsymbol{E} = \cos\psi\boldsymbol{j} + \sin\psi\boldsymbol{i}$, $\boldsymbol{i}$ and $\boldsymbol{j}$ are orthogonal unit vectors in the Cartesian coordinate system, $\boldsymbol{v}$ is the velocity, $\boldsymbol{v}_s$ is the slip velocity, and p is the pressure. Note that we use the boundary condition that the velocity on the wall of the channel is zero and that the pressures of the inlet and outlet are P_1 and P_2, respectively. (Here, $P_1 = P_2 = 0$ and $\Delta P = P_2 - P_1 = 0$.) We calculate the flow fields of the ICEP rectifier using the boundary element method on the basis of Eqs. (6)-(9).

III. RESULTS

A. Typical flow field of the ICEO rectifier

Figure 2 shows the typical flow fields of the ICEO rectifier when $y_b/w = 1.125$, $c/w = 0.2$, $\Delta P = 0$, $w = 0.1$ μm, $\bar{U}_0 = 8$ μm/s, $\Delta T = 116.2$ K, $\bar{v}_{a,rms} = 2.38$ V, and $\bar{E}_{a,rms} = 23.8$ kV/m. On one hand, for a symmetrical channel shown in Fig. 2(a), we observe a symmetrical quadrupolar electroosmotic flow around a circular metal post, and the net flow is zero (average flow velocity U_p at the inlet is zero) because the reverse flow of the left-hand part of the circular post cancels the forward flow of its right-hand part. On the other hand, for the asymmetrical channels shown in Figs. 2(b) and 2(c), we observe net flow ($U_p = 0.63$ and 0.55 μm/s, respectively) because quadrupolar electroosmotic flows around circular metal posts are asymmetrically modified by the asymmetrically structured channel. Note that the flow fields of the ICEP rectifier are similar to those of the ICEO rectifier except that $U_p = 0.80$ and 0.93 μm/s for $w_2/w_1 = 0.6$ and 0.4, respectively, and the velocities (U_y) of metal cylinders in the y direction are 0.42 and 0.81 μm/s, respectively.

B. Performance of ICEO and ICEP rectifiers

Figure 3 shows the performance of ICEO and ICEP rectifiers with a funnel channel ($w = w_1 > w_2$). Figure 3(a) shows that for the ICEP rectifier, U_p and U_y attain their maximum values of 0.94 and 0.81 μm/s at $w_2/w_1 = 0.55$ and 0.60, respectively, whereas for the ICEO rectifier, U_p increases as w_2/w_1 decreases. Figure 3(b) shows that for the ICEP rectifier, U_p and U_y attain their maximum values of 1.11 and 1.42 μm/s at $y_b/w = 1.30$ and 1.40, respectively, whereas for the ICEO rectifier, U_p attains the maximum value of 0.55 μm/s at $y_b/w = 1.10$. Figure 3(c) shows that for both ICEO and ICEP rectifiers, U_p and U_y increase as c/w increases. Note that the representative velocity $\bar{U}_0$ is proportional to c. Further, we think that U_p of the ICEP rectifier is larger than that of the ICEO rectifier because the motion of the cylinder decreases flow resistance.

C. Results for the periodic asymmetrical (ratchet-shaped) channel

Figure 4 shows the flow fields of the ICEP rectifier in the periodic asymmetrical (ratchet-shaped) channel when $L/w = 3.0$, $y_b/w = 1.3$, $x_b/w = 0.5$, $c/w = 0.2$, $\Delta P = 0$, $\bar{U}_0 = 8$ μm/s, $w = 0.1$ μm, $\bar{v}_{a,rms} = 2.38$ mV, $\Delta T = 116.2$ K, and $\bar{E}_{a,rms} = 23.8$ kV/m. Figure 5 shows the performance of the ICEO and ICEP rectifiers in the periodic asymmetrical (ratchet-shaped) channel. As shown in Fig. 5(a), U_p and U_y depend largely on c. On one hand, Fig. 5(b) shows that the ICEO rectifier works if we place the metal cylinder at a suitable position, e.g., $U_p = -1.23$ μm/s at $y_b/w = 0.90$. On the other hand, a metal cylinder or 2D metal particle of an ICEP rectifier cannot

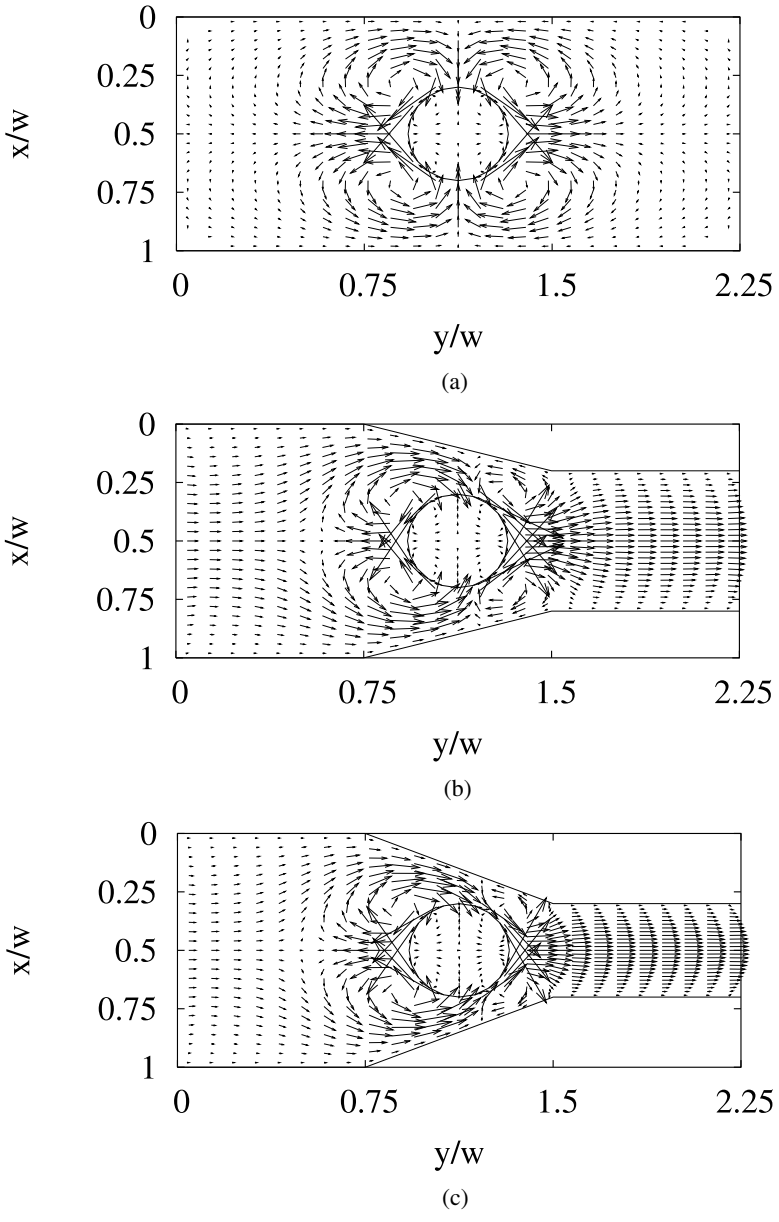

FIG. 2. Flow fields of ICEO rectifiers in a basic asymmetrical channel. Here, $y_b/w = 1.125$, $x_b/w = 0.5$, $c/w = 0.2$, $\Delta P = 0$, $\bar{U}_0 = 8$ μm/s, $w = 0.1$ μm, $\bar{v}_{a,rms} = 2.38$ mV, $\Delta T = 116.2$ K, and $\bar{E}_{a,rms} = 23.8$ kV/m. (a) $w_2/w_1 = 1.0$ ($U_p = 0.00$ μm/s). (b) $w_2/w_1 = 0.6$ ($U_p = 0.55$ μm/s). (c) $w_2/w_1 = 0.4$ ($U_p = 0.63$ μm/s).

pass through the ratchet-shaped channel because of zero and negative velocities. However, we can probably avoid this problem of an ICEP rectifier by considering a multi-particle system.

IV. DISCUSSION

A. The meaning of the rectified motion due to ICEO/ICEP

Although there is a concept of a Brownian motor that uses an asymmetrical Brownian motion resulting from random collisions with solvent molecules,[5–10] to the best of our knowledge, no report as for a fluidic rectifier that uses a thermal noise has been reported thus far. In particular, we have shown that we can explain a ratchet phenomenon qualitatively from the view point of a macroscopic design of ICEO/ICEP devices using a funnel-shaped channel. Of course, other types of ICEO/ICEP

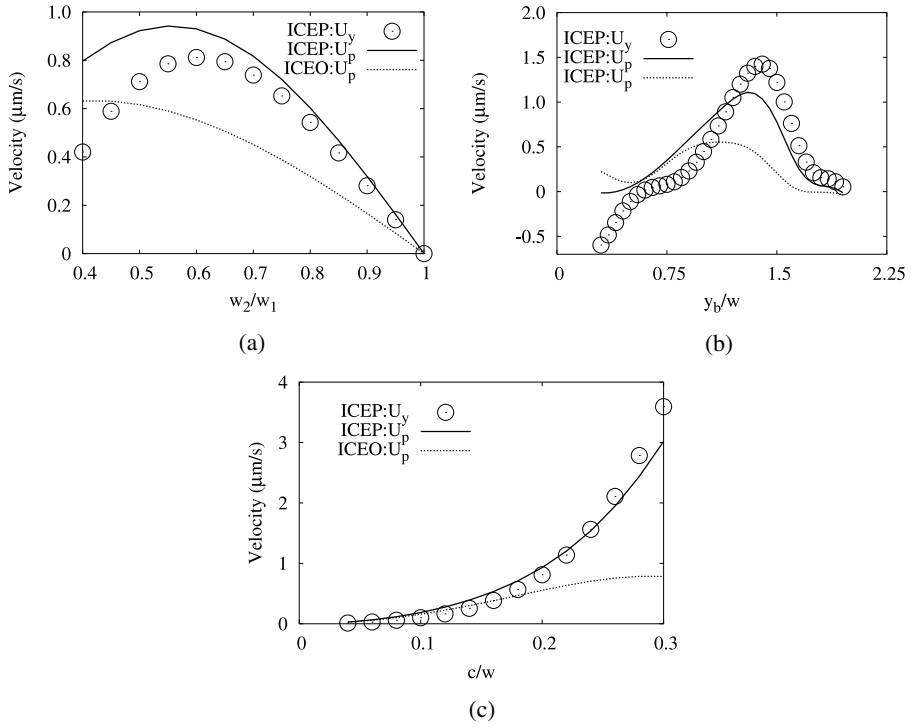

FIG. 3. Performance of ICEO and ICEP rectifiers in the basic asymmetrical channel. Here, $x_b/w = 0.5$, $\Delta P = 0$, $\bar{U}_0 = 8\ \mu$m/s, $w = 0.1\ \mu$m, $\bar{v}_{a,rms} = 2.38$ mV, $\Delta T = 116.2$ K, and $\bar{E}_{a,rms} = 23.8$ kV/m. (a) Dependence of velocities on w_2/w_1 ($y_b/w = 1.125$ and $c/w = 0.2$). (b) Dependence of velocities on y_b/w ($w_2/w_1 = 0.6$ and $c/w = 0.2$). (c) Dependence of velocities on c/w ($y_b/w = 1.125$ and $w_2/w_1 = 0.6$).

pumps (including an ac osmosis pump) can be used as the spontaneous rectifier, and we need to pursue their pumping performance.[13–21] Further, it is interesting that an observable thermal noise (∼mV) and flow ($\sim\mu$m/s) can be generated in the rectifier in the mesoscopic region even for a small temperature difference, because it can be applied to a robot, an air conditioner, etc., as a super-compact transportation system of a low energy consumption. Note that a temperature difference is also omnipresent in the world.

B. Motion due to a thermal noise

It might be surprising that a thermal noise will produce enough voltage to induce a measurable flow. However, since a rectified motion due to the thermal noise can occur only when there is a temperature difference, our predictions do not violate both the energy conservation law and the second law of

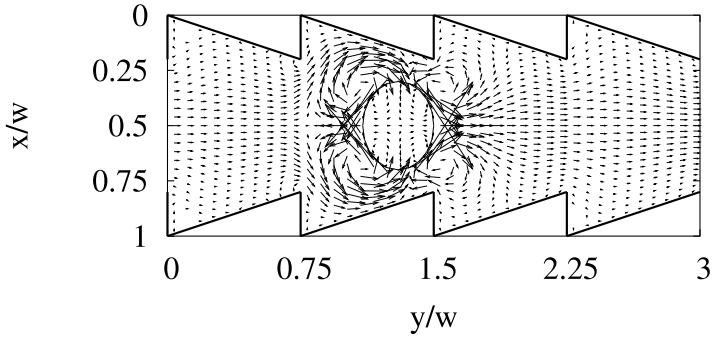

FIG. 4. Flow field of ICEP rectifier in a periodic asymmetrical (ratchet-shaped) channel. Here, $L/w = 3.0$, $y_b/w = 1.3$, $x_b/w = 0.5$, $c/w = 0.2$, $\Delta P = 0$, $\bar{U}_0 = 8\ \mu$m/s, $w = 0.1\ \mu$m, $\bar{v}_{a,rms} = 2.38$ mV, $\Delta T = 116.2$ K, and $\bar{E}_{a,rms} = 23.8$ kV/m.

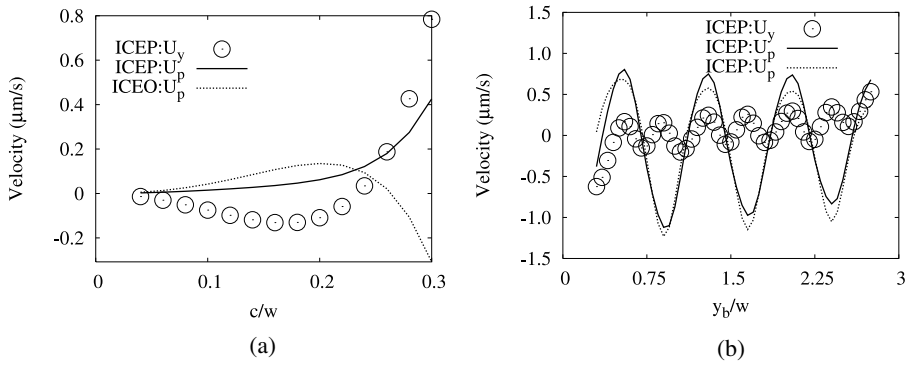

FIG. 5. Performance of ICEO and ICEP rectifiers in the periodic asymmetrical (ratchet-shaped) channel. Here, $w_2/w_1 = 0.6$, $L/w = 3.0$, $x_b/w = 0.5$, $\Delta P = 0$, $\bar{U}_0 = 8$ μm/s, $w = 0.1$ μm, $\bar{v}_{a,rms} = 2.38$ mV, $\Delta T = 116.2$ K, and $\bar{E}_{a,rms} = 23.8$ kV/m. (a) Dependence of velocities on c/w ($y_b/w = 1.125$). (b) Dependence of velocities on y_b/w ($c/w = 0.2$).

thermodynamics. Please note that from Eq. (22), the intensity of the mean square value of the applied noise voltage between electrodes becomes zero, when the temperature of Z_1 is the same as that of Z_2.

Conversely, one may think that the net ICEO/ICEP flows should be generated even when $T_1 = T_2$, since each resistance shows the thermal noise of the electric potential at any finite temperature; and the nonlinearity of ICEO/ICEP phenomena (i.e., $U_0 \propto E_a^2$) seems to provide ideal "Feynman ratchet" for the random thermal noises. Of course, the prediction is immediately rejected by the second law of thermodynamics. In fact, the thermal noise voltage between electrodes does not remain at $T_1 = T_2$, as clarified through the equivalent circuit model in Figs. 1(e) and 1(f). Namely, Eq. (13) clearly shows that the total noise current is just proportional to the excess electroforce $E_0 \equiv E_2 - E_1$. Thus, the value of the excess electroforce E_0 becomes zero at $T_1 = T_2$ since $E_2 = E_1$ at $T_1 = T_2$. Therefore, the applied noise voltage between electrodes becomes zero because of the relation that $V_a(\omega) = \frac{E_0(\omega)}{2} \frac{e^{j\theta}}{\sqrt{1+(\omega/\omega_c)^2}}$ in Eq. (15).

Further, although we mainly consider the case at $T_1 > T_2$, the formulations of Eqs. (22), (23), and (25) do not change even for the case at $T_2 < T_1$. Namely, the same rectified motion is expected even at $T_2 < T_1$. Please note that we assume that Z_1 and Z_2 are connected by the ideal electrodes of zero resistance; thus, the same thermal noise voltage ($v_a(t)$ or $V_a(\omega)$) is applied to both Z_1 and Z_2 elements.

C. Why can E_0 (=$E_1 - E_2$) induce the flow only when $\Delta T \neq 0$?

Even though we explain the rectified phenomena in detail in Secs. II D and IV B, some researchers may still insist that they cannot understand why $E_0 = E_1 - E_2$ can induce the flow only when $\Delta T \neq 0$. However, if one can understand the principle of superposition, which is the fundamental concept of an electro-circuit theory in the elementary level, the answer to the question is mathematically obvious, i.e., as described in Eq. (13), the total current I is represented by the superposition of I_1 and $-I_2$; thus, we obtain $I = (E_1 - E_2)/R_0 = E_0/R_0$ at $R_{10} = R_{20} = R_0$; therefore, obviously, only the value of E_0 (=$E_1 - E_2$) contributes the value of V_a. Namely, $E_0 = E_1 - E_2$ can induce the flow only when $\Delta T \neq 0$. In addition, although we explain in detail the reason why the noise signal at $T_1 = T_2$ cannot induce the flow from the viewpoint of the second law of thermodynamics in Secs. II D and IV B, some researchers may still insist that the flow should be induced even when $\Delta T = 0$, since the thermal noise exists as long as $T_i \neq 0$. However, we should say that the thermal noise theory is made to satisfy the second law of thermodynamics from the studies of Jonson[24] and Nyquist.[4]

D. Relation between the current theory and the thermo-kinetic theory

Furthermore, since our predictions are based on the Nyquist's traditional thermo-dynamical analysis[4] and a recent experimental fact of Callegaro and Pisani,[3] they must be reasonable. Moreover, from the viewpoint of the thermo-kinetic phenomenon,[12] the flow due to the temperature gradient

is common and we have already predicted quadrupolar thermokinetic flow around a metal cylinder under the existence of temperature gradient as a nonlinear thermokinetic phenomena.[22] Nevertheless, it is important to consider phenomena from different viewpoints, e.g., a simple noise argument here also predicts quadrupolar thermokinetic flows around a metal cylinder qualitatively at $\Delta T \neq 0$. However, different from the nonlinear thermokinetic theory[22] that predicts $\bar{U}_0 \propto |\Delta T|^2$, the simple noise argument predicts that $\bar{U}_0 \propto |\Delta T|$. Thus, we need to explore more in the future. Further, please note that the temperature difference employed in the numerical calculations ($\Delta T = 116.2$ K) is probably too large for a complete aqueous system, i.e., it might be difficult to make the temperature difference ($\Delta T = 116.2$ K) experimentally in a single aqueous channel. However, it is possible to make the temperature difference theoretically under the high pressure condition in a microfluidic channel, although it is a challenging problem. In addition, as a first experiment, we think that it is better to use a composite system consisting of the solid capacitor with small capacitance at a hot temperature (T_1) and the aqueous chamber having a metal post or metal particle at a cold temperature ($0 < T_2 < 100\,^\circ$C), since we can adjust the temperature T_1 to a high value, although it is still a challenging problem.

E. Proximity configuration

If we consider the system of $C_0 = \epsilon A/w$, $A = w^2$, $w = 0.1$ μm, and $\epsilon = 80\epsilon$, C_0 is very small ($\sim 10^{-16}$ F). Thus, matching the two capacitances C_{10} and C_{20} may imply that the rectifier is connected to the temperature reservoir by wires of dimensions similar to those of the rectifier itself. This may lead to the somewhat absurd conclusion of a ~100 K temperature difference over submicron distances since the thermophoretic experiments are typically done under the condition that $dT/dx \simeq 1$ K/μm at most.[26,27] Thus, in this case, by setting $\Delta T = 0.1$ K and $c = 0.2w$ for $w = 0.1$ μm, we obtain $\bar{U} \simeq 0.01$ μm/s from Eq. (25), as a more realistic estimation. Here, although the value of 0.01 μm/s for $\Delta T \simeq 0.1$ K is approximately 1000 times smaller than the estimation for $\Delta T \simeq 100$ K, it is still observable since the predicted flow velocity means the motion of a 1/10 characteristic length (w) per second.

In the extreme proximity condition, it is natural that the real wires are no longer required since the solution itself plays the role of wires, although the wire has the same order of the resistor, and thus, we need to consider a more sophisticated model in the future. For example, the wires should be modeled as a resistor network having a thermal noise voltage.[28] However, as a first approach, we can assume the ideal wire even for the ion conduction of the solution. This consideration leads us to the unbounded problem of a metal cylinder in an electrolyte under the temperature gradient $\sim \Delta T/w$. That is, by considering Eq. (25), $C_0 = \epsilon w$, and $c \sim w$, we obtain

$$\bar{U}_0 = \frac{\epsilon c}{\mu w^2} \bar{v}_{a,rms}^2 \simeq \frac{\epsilon w}{\mu w^2} \frac{k|\Delta T|}{4\epsilon w} \simeq \frac{k|\Delta T|}{4\mu c^2} \sim \frac{k}{4\mu c} |\nabla T|, \tag{30}$$

for the unbounded problem. From Eq. (30), the flow velocity increases as c decreases. Specifically, without the difficulty of producing a small electrode gap, we can expect the flow velocities $\bar{U} \sim 0.003\,45$, 0.0345, and 0.345 μm/s for the radii $c = 1.0$, 0.1, and 0.01 μm, respectively, at the temperature gradient $|\nabla T| = 1$ K/μm. Thus, approximately in the range $c \leq 0.1$ μm, there is a possibility to observe a quadrupolar electro-osmotic flow around the metal cylinder due to the thermal noise.

F. Callegaro-Pisani configuration

In the above discussion, we only refer to the proximity configuration due to the small capacitance C_0. However, another real motivation to use the proximity configuration is that the resistance of the rectifier (R_0) is often too large to measure. In other words, if R_0 is suitably large (approximately $0.1 \leq R_0 \leq 10$ GΩ), we can neglect the effect of small capacitance and we can separate the rectifier from the matching impedance. That is, we can use a Callegaro-Pisani configuration[3] in real experiments. Specifically, an electrical resistivity due to the bulk ion conduction[23] is provided as

$$\rho_b = \frac{\lambda_D^2}{\epsilon D}, \tag{31}$$

where D ($\simeq 10^9$ m^2/s) is the ion diffusivity, λ_D ($\equiv\sqrt{\epsilon kT/2z^2e^2C_b}$) denotes the Debye length, k is the Boltzmann constant, ze is the ion charge, T is the temperature, and C_b is the ion concentration of the bulk. Thus, we obtain $\rho_b = 1.41\times10^6$, 1.41×10^4, and 1.41×10^2 Ω m at $C_b = 10^{-7}$M, 10^{-5}M, and 10^{-3}M, respectively, i.e., $R_0 = \rho_b/w = 1.41\times10^{13}$, 1.41×10^{11}, and 1.41×10^9 at $C_b = 10^{-7}$M, 10^{-5}M, and 10^{-3}M, respectively, for $w = 0.1$ μm and $A = w^2$. Therefore, if we consider the system of $R_0 = \rho/w = 1.41$ GΩ and $C_0 = \epsilon w = 0.708\times10^{-16}$ F at $A = w^2$, $w = 0.1$ μm, $\epsilon = 80\epsilon_0$, and $C_b = 10^{-3}$M, we can neglect C_0 and we can use the Callegaro-Pisani configuration.[3] Consequently, we can obtain a large temperature difference ΔT (=217.7 K) between the rectifier at room temperature (295.0 K) and the matching impedance in a liquid nitrogen bath (77.3 K). In this case, from Eqs. (5) and (25), we obtain

$$\bar{U}_0 = \frac{\epsilon c}{\mu w^2} k\Delta T R_0 W_{band}^{eff}, \tag{32}$$

where W_{band}^{eff} is an effective band width that considers both the electrical and hydrodynamical band widths, which will be discussed in Sec. IV G. Thus, by setting $W_{band}^{eff} = 10$ kHz and $c = 0.2w$, we obtain $\bar{U}_0 = 10.6$ nm for the Callegaro-Pisani configuration. Therefore, we have a chance to observe the nonlinear electro-osmotic flow due to the thermal noise.

G. Band width of a hydrodynamic model

Our hydrodynamic model neglects the frequency dependence of the thermally driven potential. However, at frequencies above the cut-off frequency ω_c (=$1/\tau_c$) due to the charging time τ_c of an electro-double layer, the effects of surface flows will be negligible in the channel, and thus, the rectifier will fail. If we neglect the Stern condensed layer,[29] the charging time is approximately provided[23,30] as

$$\tau_c \simeq R_0 C_D \sim \frac{\lambda_D w}{D}, \tag{33}$$

where $C_D \simeq \frac{\epsilon}{\lambda_D} A$ is the capacitance of the double layer of the metal post. Thus, we obtain $\tau_c = 10^{-4}$, 10^{-5}, and 10^{-6} s at $C_b = 10^{-7}$M, 10^{-5}M, and 10^{-3}M, respectively, at $w = 0.1$ μm. Thus, the band width of an ICEO hydrodynamic model W_{band}^{hydro} is expected to be 10 kHz at least. Therefore, $W_{band}^{eff} = 10$ kHz in Sec. IV G is justified if we need not to consider the matching capacitance in the Callegaro-Pisani configuration. Further, in the proximity configuration discussed in Sec. IV F, a time constant due the electro-circuit condition is

$$\tau_e \simeq R_0 C_0 \sim \frac{\lambda_D^2}{D}. \tag{34}$$

Thus, we obtain $\tau_e = 10^{-3}$, 10^{-5}, and 10^{-7} s at $C_b = 10^{-7}$M, 10^{-5}M, and 10^{-3}M, respectively, at $w = 0.1$ μm. It means that for the proximity configuration, Eqs. (20) and (30) are reasonable at $C_b \le 0.01$ mM, whereas they overestimate a valid value at $C_b > 0.01$ mM. Please note that the concerned hydrodynamic phenomena due to a thermal noise can be observed under the condition that $c \sim w \sim \lambda_D$, as suggested by Eqs. (30) and (32). Thus, we expect that $\tau_c \sim \tau_e$ for the observable conditions, as a first approximation. In other words, the simple root mean square voltage $\bar{v}_{a,rms}$ in Eq. (23) does not include so much invalid contribution from the high frequency thermal noise for the observable conditions.

V. CONCLUSION

In conclusion, we have proposed an ICEO/ICEP rectifier that uses a thermal noise and numerically examined their performances. By the boundary element method combined with double layer approximation, we find that (1) an ICEO/ICEP rectifier having a single/multi-funnel channel can work at an observable speed (~μm/s) by the thermal voltage (~mV) with a rather small temperature difference (~100 K) for an electrode width $w = 0.1$ μm. (2) The net maximum thermal flow velocity of an ICEO/ICEP rectifier is proportional to the absolute value of the temperature difference $|\Delta T|$.

[1] L. Brillouin, "Can the rectifier become a thermodynamical demon?," Phys. Rev. **78**, 627–628 (1950).
[2] J. B. Gunn and J. L. Staples, "Spontaneous reverse current due to the Brillouin EMF in a diode," Appl. Phys. Lett. **14**, 54–56 (1969).
[3] L. Callegaro and M. Pisani, "Practical realization of Nyquists gedanken experiment," Appl. Phys. Lett. **89**, 034105 (2006).
[4] H. Nyquist, "Thermal agitation of electric charge in conductors," Phys. Rev. **32**, 110–113 (1928).
[5] M. O. Magnasco, "Forced thermal ratchets," Phys. Rev. Lett. **71**, 1477–1481 (1993).
[6] F. Jülicher, A. Ajdari, and J. Prost, "Modeling molecular motors," Rev. Mod. Phys. **69**, 1269–1282 (1997).
[7] L. Gorre-Talini, S. Jeanjean, and P. Silberzan, "Sorting of brownian particles by the pulsed application of an asymmetric potential," Phys. Rev. E **56**, 2025–2034 (1997).
[8] C. Kettner, P. Reimann, P. Hänggi, and F. Müller, "Drift ratchet," Phys. Rev. E **61**, 312–323 (2000).
[9] C. Marquet, A. Buguin, L. Talini, and P. Silberzan, "Rectified motion of colloids in asymmetrically structured channels," Phys. Rev. Lett. **88**, 168301 (2002).
[10] P. Reimann, "Brownian motors: Noisy transport far from equilibrium," Phys. Rep. **361**, 57–265 (2002).
[11] A. Groisman and S. R. Quake, "A microfluidic rectifier: Anisotropic flow resistance at low reynolds numbers," Phys. Rev. Lett. **92**, 094501 (2004).
[12] I. Goldhirsch and D. Ronis, "Theory of thermophoresis. I. General considerations and mode-coupling analysis," Phys. Rev. A **27**, 1616 (1983).
[13] M. Bazant and T. Squires, "Induced-charge electrokinetic phenomena: Theory and microfluidic applications," Phys. Rev. Lett. **92**, 066101 (2004).
[14] T. Squires and M. Bazant, "Induced-charge electro-osmosis," J. Fluid Mech. **509**, 217 (2004).
[15] J. P. Urbanski, T. Thorsen, J. A. Levitan, and M. Z. Bazant, "Fast ac electro-osmotic micropumps with nonplanar electrodes," Appl. Phys. Lett. **89**, 143508 (2006).
[16] D. Burch and M. Z. Bazant, "Design principle for improved three-dimensional ac electro-osmotic pumps," Phys. Rev. E **77**, 055303 (2008).
[17] S. Gangwal, O. Cayre, M. Bazant, and O. Velev, "Induced-charge electrophoresis of metallodielectric particles," Phys. Rev. Lett. **100**, 058302 (2008).
[18] A. Ramos, A. González, A. Castellanos, N. G. Green, and H. Morgan, "Pumping of liquids with ac voltages applied to asymmetric pairs of microelectrodes," Phys. Rev. E **67**, 056302 (2003).
[19] A. Ajdari, "Pumping liquids using asymmetric electrode arrays," Phys. Rev. E **61**, R45–R48 (2000).
[20] L. H. Olesen, H. Bruus, and A. Ajdari, "ac electrokinetic micropumps: The effect of geometrical confinement, Faradaic current injection, and nonlinear surface capacitance," Phys. Rev. E **73**, 056313 (2006).
[21] H. Sugioka, "Suppression of reverse flows in pumping by induced-charge electro-osmosis using asymmetrically stacked elliptical metal posts," Phys. Rev. E **78**, 057301 (2008).
[22] H. Sugioka, "Nonlinear thermokinetic phenomena due to the seebeck effect," Langmuir **30**, 8621 (2014).
[23] M. Z. Bazant, K. Thornton, and A. Ajdari, "Diffuse-charge dynamics in electrochemical systems," Phys. Rev. E **70**, 021506 (2004).
[24] J. B. Johnson, "Thermal agitation of electricity in conductors," Phys. Rev. **32**, 97–109 (1928).
[25] M. Fair and J. Anderson, "Electrophoresis of non-uniformly charged ellipsoidal particles," J. Colloid Interface Sci. **127**, 388 (1989).
[26] H. Jiang, N. Yoshinaga, and M. Sano, "Active motion of a janus particle by self-thermophoresis in a defocused laser beam," Phys. Rev. Lett. **105**, 268302 (2010).
[27] H. Jiang, H. Wada, N. Yoshinaga, and M. Sano, "Manipulation of colloids by a nonequilibrium depletion force in a temperature," Phys. Rev. Lett. **102**, 208301 (2009).
[28] T. Varpula and T. Poutanen, "Magnetic field fluctuations arising from thermal motion of electric charge in conductors," J. Appl. Phys. **55**, 4015–4021 (1984).
[29] A. J. Pascall and T. M. Squires, "Induced charge electro-osmosis over controllably contaminated electrodes," Phys. Rev. Lett. **104**, 088301 (2010).
[30] H. Sugioka, "High-speed rotary microvalves in water using hydrodynamic force due to induced-charge electrophoresis," Phys. Rev. E **81**, 036301 (2010).